Authors' version
presented at the IEEE/ASME International Conference on Advanced Intelligent Mechatronics (AIM) 12-16 July, 2021. DOI: 10.1109/AIM46487.2021.9517659

Design and Evaluation of a Series-Elastic Gyroscopic Actuator for Balance Assistance

1st Charlotte Marquardt
Institute of Anthropomatics and Robotics,
Karlsruhe Institute of Technology
Karlsruhe, DE
charlotte.marquardt@kit.edu

2nd Daniel Lemus
Department of Rehabilitation Medicine,
Erasmus MC, Rotterdam, NL
& Delft University of Technology, Delft, NL
d.lemusperez@erasmusmc.nl

3rd Cory Meijneke
Electrical and Mechanical Support Division
Delft University of Technology
Delft, NL
c.meijneke@tudelft.nl

4th Heike Vallery
Department of BioMechanical Engineering,
Delft University of Technology, Delft, NL
& Erasmus MC, Rotterdam, NL
h.vallery@tudelft.nl

***Abstract*—Sensory-motor impairments due to age or neurological diseases can influence a person's ability to maintain balance, and increase the risk of falls. Recently, wearable Control Moment Gyroscopes (CMGs) have proven to provide effective balance support. Here, we show a new design of a Series-Elastic Control Moment Gyroscope (SECMG) enhanced by an additional passive degree of freedom, namely a second, orthogonal gimbal that is supported by a (visco)elastic element. The design mainly aims to reject disturbances originating from human movement and render a low remaining impedance, as well as to provide more accurate torque sensing, based on angular deflection of the compliant element. Evaluation of the torque tracking performance with regards to a classic rigid Single-Gimbal Control Moment Gyroscope (SGCMG) showed that the device equally exceeds the bandwidth requirements for its application in human augmentation. However, characterization of our current compliant construction also revealed some backlash occluding the torque-deflection relation. In the future, the SECMG could be evaluated in experiments with humans, to validate its predicted low remaining impedance.**

***Index Terms*—control moment gyroscope, CMG, series-elastic actuator, SEA, wearable robotics, torque control.**

I. Introduction

MOBILITY and therefore often independence depends on balance [1], which characterizes the ability to use body posture to prevent falling [2]. Impairments in the sensory-motor system, due to factors such as age and neurological diseases, can reduce the ability to maintain balance when performing a range of functional tasks of daily life, which leads to a higher occurrence of falls [1], [3].

Control Moment Gyroscopes already occupy a prominent place in aerospace applications, such as spacecrafts and space suits [4], [5], but only recently have they received more attention in terrestrial applications, for example in marine vehicles [6], [7] or human balance assistance [8], [9]. In previous publications [8], [10], we presented a first prototype that effectively assists balance, with feedback control only based on inertial upper-body sensors. The single actuator can provide stability in either the sagittal or frontal plane independently, which shows the potential of such devices for rehabilitation.

In applications of CMGs involving direct human interaction, often in unstructured environments, torques have to be transmitted safely. An option to decouple actuator inertia from the load can be found in Series-Elastic Actuators (SEAs). Despite their drawbacks such as limited torque tracking bandwidth and stability, SEAs offer several advantages, including low realizable impedance, shock compensation and the possibility to function as low-cost force sensors, relying on the force-elongation relationship of the elastic element [11]–[13]. The inclusion of viscoelastic materials in SEAs enhances control stability via intrinsic damping, but this also introduces hysteretic effects that can hamper sensing. State observers capturing this more complex behavior have proven successful to overcome the limitations, particularly the hysteresis for both linear [14]–[16] and non-linear viscoelastic materials [17] and thus also allow viscoelastic materials to be used as reliable force sensors.

This paper presents a SECMG (Fig. 1), tailored to the requirements of a wearable device.

Fig. 1. One of the authors wearing the device.

Compared to our first prototype [8], this second prototype has an additional Degree of Freedom (DoF), an inner gimbal. This passive DoF incorporates a compliant element, and it also allows completely decoupling the flywheel's orientation from the user, to ensure safety by halting any transmission of moments. The passive compliance attempts to serve as torque sensor, reduce minimal realizable impedance, and generally improve torque control. Further improvements include infinite rotation of the outer gimbal frame, compared to the restricted range of motion of the first prototype. Furthermore, the system features a flywheel with a shape more adjusted to transmitting gyroscopic moments.

In Section II, we present the design of the device. Section III gives an overview about the experimental setup and the signals used to evaluate the performance of the SECMG in comparison to a rigid (single-gimbal) version of the device. The results are presented in Section IV. Section V discusses all results and future work and in Section VI we draw a conclusions from our findings.

II. Design

A. Mechanical Design

The inner gimbal (see Fig. 2 bottom) consist of a hollow bicone flywheel in a spherical partial vacuum chamber capable of applying a vacuum up to 200 mbar. The design by Hyperion Technologies leads to a higher angular momentum due to a higher moment of inertia and reduced friction. The flywheel is actuated by a Thingap outrunner 151 W motor (TG3053) which can reach velocities of 12.000 rpm and is controlled by an ELMO Gold Twitter 10/100 servo drive. The position of the motor is measured by an RLS RLC2IC encoder with a resolution of 7200 cpt. Suitable suspension is achieved by two super precision angular contact bearings (NSK 7909C) with LGLT 2 lubrication.

The outer gimbal case (see Fig. 2 top) around the flywheel is actuated by a brushless Maxon EC 45 flat Ø42.8 mm 70 W motor. Another ELMO Gold Twitter 10/100 servo drive controls the gimbal motor. A harmonic drive (Leaderdrive LHSG-14-80-C-II) with a gear ratio of 80:1 increases the transmitted torque. A RLS 14 bit orbis absolute encoder allows measurements of the gimbal position. A cylindrical slipring (Moflon MMC182) on the bottom of the device allows unconstrained infinite gimbal rotation and real-time transfer of sensor data out of the inner gimbal. An element consisting of the curved jaw of a Lovejoy SPIDEX® coupling in a custom-made hub is added on the gyroscopic output axis (see Fig. 3 right) to decouple the load from the actuator without significant losses to the generated gyroscopic output torque, similar to a SEA. The deflection angle is registered by another RLS 14 bit orbis absolute encoder. The complete prototype including its backpack structure weighs 10.8 kg, thus being within the range of other existing wearable balance-assisting devices [9], [10], [18], other than the much lighter CMG by [19].

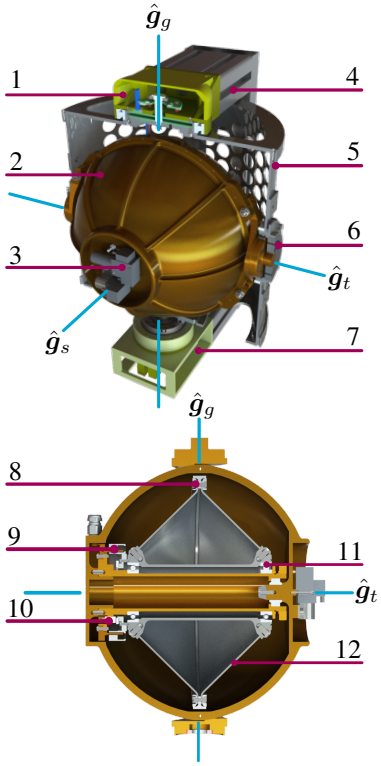

Fig. 2. The top figure shows a semi-cross-section of the whole device where (1) denotes the housing for the slip-ring and gimbal encoder, (2) the vacuum housing, (3) the vacuum-pump, (4) the device-frame, (5) the gimbal-frame, (6) the series coupling, and (7) the gimbal motor and gearbox. The bottom figure shows a cross-section of the sphere where (8) denotes the flywheel rim, (9) the electric motor, (10) The flywheel encoder, (11) the bearings, (12) the flywheel-sides.

B. Control and Communication

Communication is handled via an EtherCAT protocol. The hardware architecture comprises a desktop target PC with Linux RT as an EtherCAT master, which runs the compiled firmware from MATLAB R2018b Simulink® and two EtherCAT slaves (motor drives), which execute the firmware on the device itself. The supervision tool TestManager by EtherLAB on a separate computer (Host PC) is used to remotely monitor and interact with the controller.

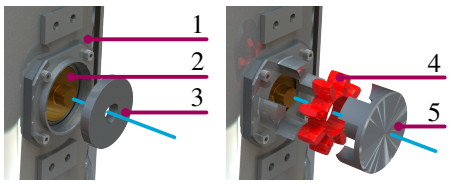

Fig. 3. Figure of the three options on the series coupling, where (1) is the gimbal frame and (2) the vacuum housing. Components (2) is rotationally contained via a P3G connection (acc. DIN 32711). Bottom left shows the locked option, where (3) is a solid disk. Bottom right is the viscoelastic option where (4) is the elastomer element and (5) the hub.

The general proposed control architecture (Fig. 4) comprises three different control levels. The controller of the highest level (green) detects the loss of balance of the wearer and keeps the wearer balanced. This high-level controller provides the reference torque $M_{\mathrm{CMG,ref}}$ online (in analogy to [10]), which is tracked by a torque controller in the middle layer (blue), resulting in the reference gimbal velocity $\dot{\gamma}_{\mathrm{ref}}$. Within the low-level control (orange), a PI controller ensures tracking of the commanded gimbal velocity $\dot{\gamma}_{\mathrm{ref}}$. A similar PI controller ensures constant flywheel velocity Ω.

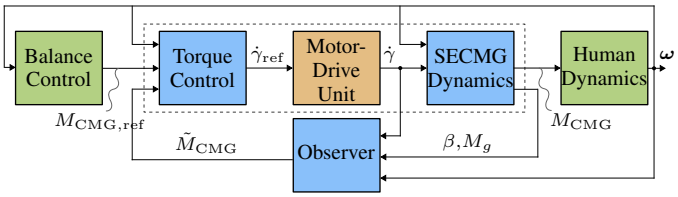

Fig. 4. Proposed observer-based control approach. The dashed box highlights the scope of this paper.

An observer provides the approximated gyroscopic output torque $\tilde{M}_{\mathrm{CMG}}$, based on the gimbal velocity, the deflection angle β of the compliant gimbal, and human motion.

For the torque controller in the middle layer, the SECMG could in principle be modeled as a Double-Gimbal Control Moment Gyroscope (DGCMG), because of its second, inner gimbal frame. However, its principle of operation resembles more that of a SGCMG, because the inner gimbal frame is constrained by the compliant element. As we allow only small deflections of the inner gimbal, we approximate its dynamics as a SGCMG.

III. Evaluation

A. Experimental Setup

In the experimental setup (Fig. 5), the SECMG is rigidly mounted on a compact multi-component sensor (HBM K-MCS10-010-6C) on a table. Signals are processed through a set of six strain gauge amplifiers implemented as six additional EtherCAT slaves. The flywheel reference velocity Ω_{ref} is set to a constant value of 800 $^{\mathrm{rad}}/_{\mathrm{s}}$ to reach a peak torque of approximately 15 N m in combination with the gimbal motion, as we have recently shown that this is sufficient to assist human balance [10]. The flywheel and gimbal velocity (Ω, $\dot{\gamma}$) and the angular deflection of the elastic element β are obtained from the corresponding motor drives and encoders.

To compare the behavior of the device in its compliant configuration to a rigid configuration, we repeated all experiments with a firmly secured output axis (Fig. 3 left).

B. Reference Signals

In the absence of human movement and with constant flywheel speed, the output torque tracking task translates into the tracking of a gimbal reference velocity. In the case of the stationary experimental setup, neglecting any motion from the user or perturbations of the environment, the reference

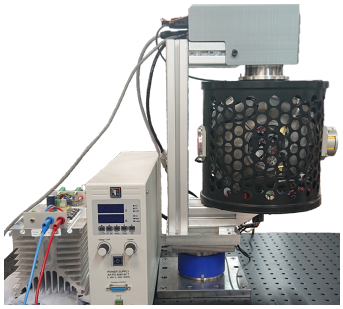

Fig. 5. Stationary experimental setup, where the SECMG is located on top of a multi-component sensor.

gyroscopic output torque $M_{\mathrm{CMG,ref}}$ about the $\hat{\boldsymbol{g}}_t$ axis is related to the reference gimbal velocity via

$$M_{\mathrm{CMG,ref}} = J_s \Omega \dot{\gamma}_{\mathrm{ref}}, \tag{1}$$

with the flywheel moment of inertia J_s [20].

Torque tracking performance was thus evaluated by subjecting the device to a sinusoidal reference gimbal velocity $\dot{\gamma}_{\mathrm{ref}}$ with an amplitude of 4 $^{\mathrm{rad}}/_{\mathrm{s}}$ and with frequencies from 0.01 Hz to 10 Hz, which increased each decade by 0.01 Hz to 0.1 Hz respectively. The amplitude was chosen according to the available maximum acceleration (10 $^{\mathrm{rad}}/_{\mathrm{s}^2}$). We applied two oscillations per frequency to allow the system to settle into quasi steady-state. The frequency response was analyzed by only fitting the second oscillation of the signal at each frequency to avoid artifacts at each frequency transition.

To analyze the viscoelastic behavior and the resulting torque-deflection relation of the SPIDEX®, we used two consecutive reference gimbal velocity pulses in both directions with a magnitude of 4 $^{\mathrm{rad}}/_{\mathrm{s}}$ as input for the device. Dynamic retardation was analyzed using the same multisine as input as stated above for the torque tracking performance.

C. Signal Processing

For stability and tracking performance reasons [21], [22], all signals were recorded using a sample frequency of 1 kHz and post-processed using MATLAB 2020a [23]. After removing small sensor bias, the load cell torque components were transformed into the gimbal frame via the rotation matrix of the gimbal position γ to obtain the gyroscopic output torque about the $\hat{\boldsymbol{g}}_t$ axis. The estimated gyroscopic output torque $M_{\mathrm{CMG,est}}$ was calculated in analogy to (1), but based on the gimbal velocity $\dot{\gamma}_{enc}$, as measured by the absolute encoder.

In order to allow for a better visualization in the plots, the signals were filtered using a second-order Butterworth filter with a cut-off frequency of 50 Hz for the frequency analysis and 10 Hz for the viscoelastic characterization, selected manually by visual inspection. The filter was applied bi-directional to allow for zero phase distortion. The underlying analysis of the frequency response and the dynamic retardation was based on the raw, unfiltered data from the multisine.

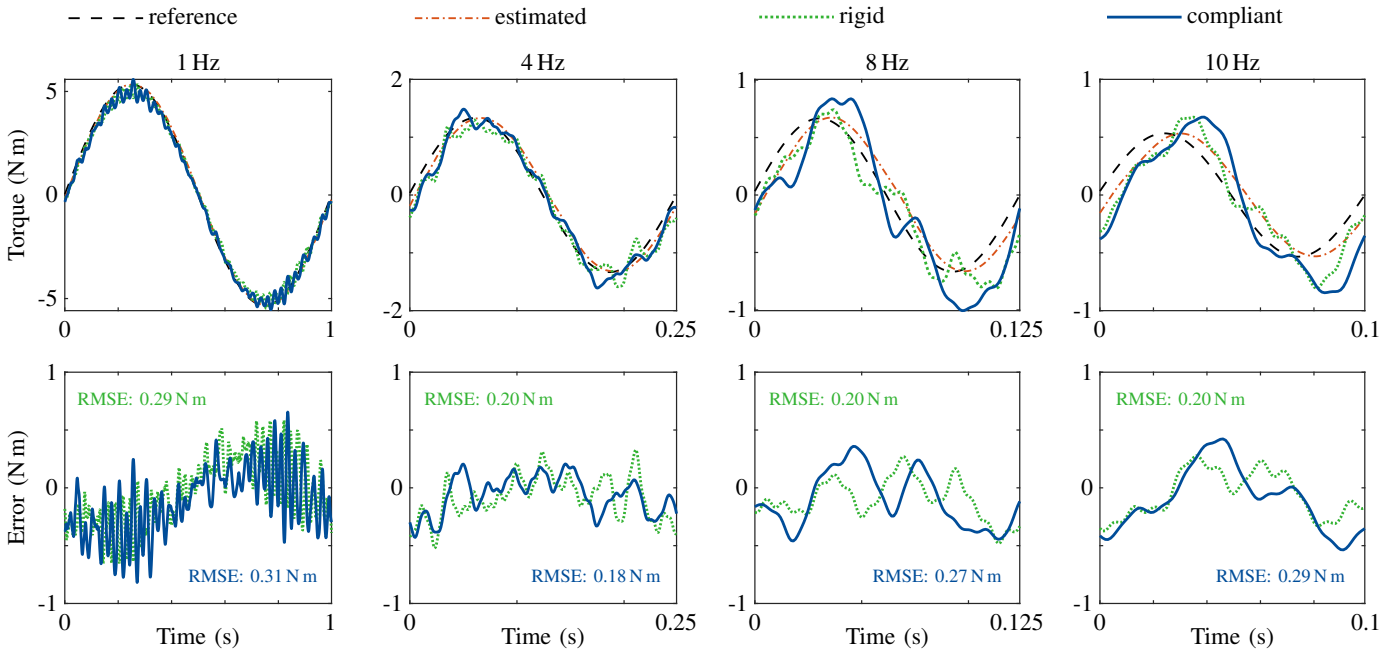

Fig. 6. Reference, estimated and both measured load cell torques of the compliant and rigid CMG at 1 Hz, 4 Hz, 8 Hz and 10 Hz, as well as the error between each load cell torque and the reference torque.

IV. Results

A. Torque Tracking Behavior

Fig. 7 shows similar frequency response results for both configurations, rigid and compliant. The phase angle is constant at about 0° up to about 1 Hz, and then decreases to about −30° at 10 Hz. The magnitude is constant at about −0.25 dB up to about 5 Hz and shows stronger variations and a small increase for higher frequencies. Fig. 6 displays the reference, estimated and measured gyroscopic torques at 1 Hz, 4 Hz, 8 Hz and 10 Hz.

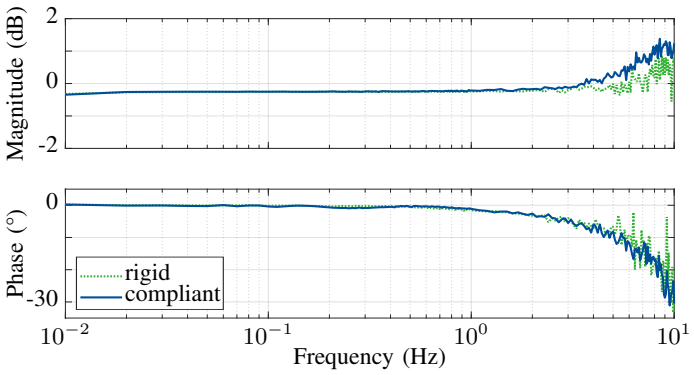

Fig. 7. Frequency response of the compliant and rigid CMG with respect to the multisine reference torque.

B. Viscoelastic Behavior

The material of the SPIDEX® exhibits at the beginning of each pulse instantaneous and towards the end of the pulse slightly delayed elasticity and recovery visible in the exemplary torque pulse test (Fig. 8) showing the torque tracking behavior for one single pulse in each direction and the corresponding angular deflection. We also observed a strong symmetrical permanent set of about 0.01 rad in its relaxation state. Both effects lead to a nonlinear torque-deflection behavior with a hysteresis shown in Fig. 9.

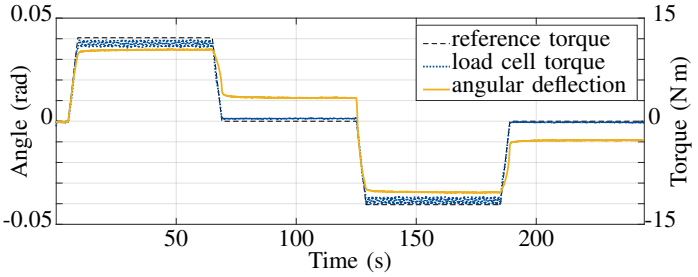

Fig. 8. Exemplary torque pulse experiment showing the torque tracking ability and the resulting angular deflection.

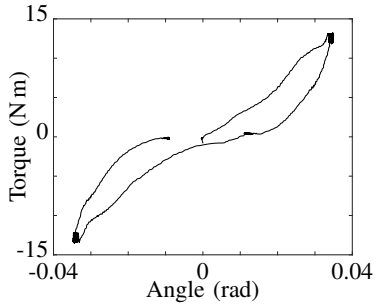

Fig. 9. Torque-deflection relation of the SPIDEX®

The dynamic retardation is displayed in Fig. 10 as the difference in phase of the frequency response of the angular deflection and the gyroscopic output torque. The SPIDEX® shows a slightly decreasing retardation angle, beginning at about $-10°$ up to 0.4 Hz, which decreases more strongly with an increased noise for higher frequencies.

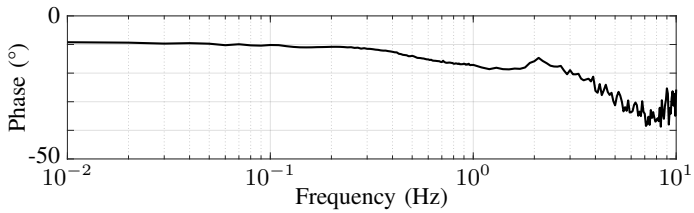

Fig. 10. Dynamic retardation of the viscoelastic material represented as the difference in phase of the frequency response of the angular deflection and the gyroscopic output torque.

V. Discussion

A. Torque Tracking Performance and Sensing Limitations

Comparing the frequency response of the compliant and the rigid CMG, the inclusion of a viscoelastic element does not appear to reduce performance. Taking into account the standard physiological time delay of about 150 ms to 200 ms in human postural control [24], [25], both configurations exceed the bandwidth requirements for application in human balance assistance. So, integration of series-(visco)elasticity in a CMG seems to be applicable without a relevant limitation of bandwidth.

However, the stationary experimental setup limits conclusions regarding the wearable application, particularly regarding the influence of human motion or other unpredictable perturbations of the environment. The human upper body's angular velocity vector has to be considered when controlling the device, as it is expected to affect the torque tracking performance as well as the accuracy of the torque estimation. Under those circumstances, the dedicated viscoelastic torque sensing is expected to show a key advantage compared to the model-based torque estimation using gimbal velocity.

Further effects due to the slight deflection of the inner gimbal while modeling the system as a SGCMG instead of a DGCMG can be neglected. Any losses in the gyroscopic output torque due to the simplified model are very small ($1 - \cos(\beta) \approx 0$), approx. 0.8 % at a maximum angular deflection of the inner gimbal of $\beta = \pm 0.04\,\mathrm{rad}$.

B. Viscoelastic Characterization

SEAs traditionally make use of the elastic element also as a cheap sensor, based on deflection. However, in contrast to more conventional SEAs, we used a viscoelastic material, aiming to provide intrinsic damping. But the characterization of the torque-deflection characteristic of the SPIDEX® proved to be difficult. A permanent set limited the possibilities of determining an accurate model for torque estimation. Likely source of the observation is a small clearance in the mount of the coupling and between the elements of the coupling itself. This backlash amplifies the non-linearity and the hysteretic effect and thus complicates detecting and estimating torque accurately for small angular deflections.

Even though the backlash appears large compared to the angular deflection, it did not appear to have a strong effect on the torque tracking performance, due to the large amplitude of the sinusoidal gyroscopic output torque.

Overall, the high stiffness of the SPIDEX® prevents substantial reduction of the gyroscopic output torque, but it also limits sensitivity regarding small gyroscopic output torques that lead to very small angular deflections.

C. Future Work

One aim of the inclusion of an elastic element in series in a CMG was to improve torque sensing. To achieve this, a reduction of the backlash in the mechanical design should be primarily aimed for, to increase accuracy of a future torque observer based on linear viscoelastic theory.

Furthermore, as a shortcoming in the experiments, the investigations of the output torque characteristics of a SECMG containing a traditional spiral spring with a linear characteristic compared to the introduced viscoelastic SECMG to illustrate the potential advantage of the material of the SPIDEX remain to be considered.

A further key benefit of including the additional degree of freedom is that the axis could in principle be decoupled, such that (if the gimbal motor generates no torque either) the flywheel always maintains its absolute orientation in space, and no gyroscopic moment is transmitted in response to human movement. This would require using a clutching element that can vary the torque transmitted, for example in the form of an overload clutch, or in the form of a controllable clutch. Commercial electromechanical clutches, however, are rather heavy and bulky for the intended wearable purpose. In another submission to this conference [26], we therefore investigated the potential of rotary electroadhesive clutches for this purpose, which could offer controllable clutching torque with minimal volume and mass.

Experimental evaluation of the potential benefits of a SECMG with regards to its realizable impedance and shock rejection abilities remains to be addressed. Similar to the first prototype [8], the experiments for human subjects wearing the SECMG to adjust body posture and maintain balance are expected to validate the actual effect of SECMG for balance assistance.

VI. Conclusion

We presented a Series-Elastic Control Moment Gyroscope, which includes an additional passive inner gimbal within a SGCMG. This inner gimbal integrates an axial-symmetric viscolastic element in series to the gyroscopic output axis. Comparison with a rigid configuration of the device similar to a SGCMG in a stationary experimental setup showed comparable performance without reduction of bandwidth due to the inclusion of series-elasticity. Moreover, the device

exceeds bandwidth requirements of its application in human augmentation at about 5 Hz.

Characterization of the viscoelastic material to enable it as an active torque sensor revealed a non-linear torque-deflection relation and a hysteresis, which is likely due to backlash in the mechanical components. Even though the high stiffness of the chosen material prevents relevant losses to the gyroscopic output torque, it exacerbates the effect of backlash on the deflection-based torque sensing. Therefore, future work is needed to reduce this effect.

Overall, the concept of a SECMG appears feasible, but it has to be determined if the benefits outweigh its limitations not only regarding the inclusion of a viscoelastic material, but also the added mass and envelope due to the required additional gimbal.

ACKNOWLEDGMENT

This research was supported by the U.S. Department of Education, National Institute on Disability and Rehabilitation Research, NIDRR-RERC, Grant No. H133E120010 and the Innovational Research Incentives Scheme Vidi with Project No. 14865, from The Netherlands Organization for Scientific Research (NWO). Charlotte Marquardt was supported by an ERASMUS+ traineeship grant and by the INOPRO project (16SV7665) funded by the German Federal Ministry of Education and Research (BMBF) .

The authors would like to thank Saher Jabeen, Andrew Berry, Andries Oort, Giel Hermans, Jan van Frankenhuyzen, and Hyperion Technologies B.V. for their contributions to this work over the years and Tamim Asfour for the overall support.

SUPPLEMENTARY MATERIALS

In order to allow verification and review of our data and code, we have uploaded the resources to an open-access public repository available in the 4TU.ResearchData [23].

REFERENCES

[1] H. Stolze, S. Klebe, C. Zechlin, C. Baecker, L. Friege, and G. Deuschl, "Falls in frequent neurological diseases," *Journal of Neurology*, vol. 251, pp. 79–84, Jan 2004.

[2] D. Winter, "Human balance and posture control during standing and walking," *Gait & Posture*, vol. 3, no. 4, pp. 193 – 214, 1995.

[3] K. Delbaere, C. Sherrington, and S. R. Lord, "Falls prevention interventions," in *Osteoporosis (Fourth Edition)*, R. Marcus, D. Feldman, D. W. Dempster, M. Luckey, and J. A. Cauley, Eds. San Diego: Academic Press, 2013, pp. 1649 – 1666.

[4] F. A. Leve, B. J. Hamilton, and M. A. Peck, *Spacecraft Momentum Control Systems*, ser. Space Technology Library. Springer, 2015, vol. 34.

[5] R. A. Vasquez, M. L. Hansberry, K. R. Duda, A. J. Middleton, and D. J. Newman, "Wearable cmg design for the variable vector countermeasure suit," in *IEEE Aerospace Conference*, March 2015, pp. 1–13.

[6] N. Townsend, A. Murphy, and R. Shenoi, "A new active gyrostabiliser system for ride control of marine vehicles," *Ocean Engineering*, vol. 34, no. 11, pp. 1607–1617, 2007.

[7] A. K. Poh, C. H. Tang, H. Kang, K. Lee, C. Siow, A. M. A. Malik, and M. Mailah, "Gyroscopic stabilisation of rolling motion in simplified marine hull model," in *IEEE International Conference on Underwater System Technology: Theory and Applications (USYS)*, 2017.

[8] D. Lemus, J. van Frankenhuyzen, and H. Vallery, "Design and Evaluation of a Balance Assistance Control Moment Gyroscope," *Journal of Mechanisms and Robotics*, vol. 9, no. 5, 08 2017.

[9] J. Chiu and A. Goswami, "Design of a Wearable Scissored-Pair Control Moment Gyroscope (SP-CMG) for Human Balance Assist," in *International Design Engineering Technical Conferences and Computers and Information in Engineering Conference*, vol. Volume 5A: 38th Mechanisms and Robotics Conference, 08 2014.

[10] D. Lemus, A. Berry, S. Jabeen, C. Jayaraman, K. Hohl, F. C. T. van der Helm, A. Jayaraman, and H. Vallery, "Controller synthesis and clinical exploration of wearable gyroscopic actuators to support human balance," *Scientific Reports*, vol. 10, Jun. 2020.

[11] G. A. Pratt and M. M. Williamson, "Series elastic actuators," in *IEEE/RSJ International Conference on Intelligent Robots and Systems. Human Robot Interaction and Cooperative Robots*, vol. 1, Aug 1995, pp. 399–406 vol.1.

[12] J. Pratt, B. Krupp, and C. Morse, "Series elastic actuators for high fidelity force control," *Industrial Robot: An International Journal*, vol. 29, no. 3, pp. 234–241, 2002.

[13] H. Vallery, R. Ekkelenkamp, H. van der Kooij, and M. Buss, "Passive and accurate torque control of series elastic actuators," in *IEEE/RSJ International Conference on Intelligent Robots and Systems*, Oct 2007, pp. 3534–3538.

[14] F. Parietti, G. Baud-Bovy, E. Gatti, R. Riener, L. Guzzella, and H. Vallery, "Series viscoelastic actuators can match human force perception," *IEEE/ASME Transactions on Mechatronics*, vol. 16, no. 5, pp. 853–860, Oct 2011.

[15] S. Pfeifer, A. Pagel, R. Riener, and H. Vallery, "Actuator with angle-dependent elasticity for biomimetic transfemoral prostheses," *IEEE/ASME Transactions on Mechatronics*, vol. 20, no. 3, pp. 1384–1394, June 2015.

[16] J. W. Hurst, A. A. Rizzi, and D. Hobbelen, "Series elastic actuation: Potential and pitfalls," *Proc. Int. Conf. Climbing Walking Robots*, p. 1–6, 2004.

[17] J. Austin, A. Schepelmann, and H. Geyer, "Control and evaluation of series elastic actuators with nonlinear rubber springs," in *IEEE/RSJ International Conference on Intelligent Robots and Systems (IROS)*, Sep. 2015, pp. 6563–6568.

[18] P. Romtrairat, C. Virulsri, P. Wattanasiri, and P. Tangpornprasert, "A performance study of a wearable balance assistance device consisting of scissored-pair control moment gyroscopes and a two-axis inclination sensor," *Journal of Biomechanics*, vol. 109, Aug. 2020.

[19] C. Meijneke, B. Sterke, G. Hermans, W. Gregoor, H. Vallery, and D. Lemus, "Design and evaluation of pint-sized gyroscopic actuators," in *IEEE/ASME International Conference on Advanced Intelligent Mechatronics (AIM) (accepted)*, 2021.

[20] H. Schaub, S. R. Vadali, J. L. Junkins *et al.*, "Feedback control law for variable speed control moment gyros," *Journal of the Astronautical Sciences*, vol. 46, no. 3, pp. 307–328, 07 1998.

[21] P. Hinterseer, S. Hirche, S. Chaudhuri, E. Steinbach, and M. Buss, "Perception-based data reduction and transmission of haptic data in telepresence and teleaction systems," *IEEE Transactions on Signal Processing*, vol. 56, no. 2, pp. 588–597, 2008.

[22] S. Hirche and M. Buss, "Transparent Data Reduction in Networked Telepresence and Teleaction Systems. Part II: Time-Delayed Communication," *Presence: Teleoperators and Virtual Environments*, vol. 16, no. 5, pp. 532–542, 10 2007. [Online]. Available: https://doi.org/10.1162/pres.16.5.532

[23] C. Marquardt, D. Lemus, C. Meijneke, and H. Vallery, "Supplementary Data on Design and Evaluation of a Series-Elastic Gyroscopic Actuator for Balance Assistance," https://data.4tu.nl/articles/dataset/Design_and_Evaluation_of_a_Series-ElasticGyroscopic_Actuator_for_Balance_Assistance/14625855, 2021.

[24] R. J. Peterka, "Sensorimotor integration in human postural control," *Journal of Neurophysiology*, vol. 88, no. 3, pp. 1097–1118, 2002.

[25] B. S. Davidson, M. L. Madigan, S. C. Southward, and M. A. Nussbaum, "Neural control of posture during small magnitude perturbations: Effects of aging and localized muscle fatigue," *IEEE Transactions on Biomedical Engineering*, vol. 58, no. 6, pp. 1546–1554, 2011.

[26] A. Detailleur, S. Umans, H. V. Even, and H. Vallery, "Feasibility analysis of a self-reinforcing, electroadhesive, rotational clutch," in *IEEE/ASME International Conference on Advanced Intelligent Mechatronics (AIM) (accepted)*, 2021.